IJCRT.ORG ISSN : 2320-2882

INTERNATIONAL JOURNAL OF CREATIVE RESEARCH THOUGHTS (IJCRT)

An International Open Access, Peer-reviewed, Refereed Journal

Study Of Hall Current Effects on MHD Convective Flow of Fluid with Thermal Radiation

Sumeet Upadhyay[1] , Prof.(Dr.) Hrishikesh Pandey[2]

[1]Research Scholar Department Of Mathematics Jai Prakash University Chapra

[2]Department Of Mathematics, Kamla Rai College Gopalganj, Jai Prakash University Chapra

Introduction

An analysis of the magnetohydrodynamic (MHD) unsteady convective flow of a viscoelastic (second grade) fluid through a porous medium filled in a vertical channel is carried out. One of the porous plates of the channel through which the fluid is injected is subjected to a slip-flow condition and the other through which the fluid is sucked to a no-slip condition. The pressure gradient in the channel varies periodically with time. The entire system rotates in unison about an axis perpendicular to the planes of the channel plates. The fluid is electrically conducting, and a magnetic field of uniform strength is applied along the axis of rotation. The non-uniform temperature difference of the plates is high enough to induce heat radiation. Assuming constant injection/suction at the channel plates, a closed form solution of the equations governing the flow is obtained. The effects of rotation, Hall current, slipflow parameter, viscoelastic parameter, Grashof number, Reynolds number, the permeability of the porous medium, etc. are shown graphically on the velocity and skin friction and discussed in detail.

In the recent past, considerable attention has been gained by the magnetohydrodynamic (MHD) rotating flows of electrically conducting, viscoelastic incompressible fluids due to its numerous applications in the cosmic and geophysical fluid dynamics. The subject of geophysical dynamics nowadays has become an important branch of fluid dynamics due to the increasing interest to study environment. In astrophysics, it is applied to study the stellar and solar structure, interplanetary and interstellar matter, solar storms and flares, etc. During the last few decades, it also finds its application in engineering. Among the applications of rotating flow in porous media to engineering disciplines, one can find the food processing industry, chemical process industry, centrifugation and filtration processes and rotating machinery. In recent years a number of studies have also appeared in the literature on the fluid phenomena on earth involving rotation to a greater or lesser extent viz. Singh (2000) analyzed the oscillatory magnetohydrodynamic (MHD) Couette flow in a rotating system in the presence of a transverse magnetic field. [1]

Basic equations

The equations governing the unsteady MHD convective flow of an incompressible, viscoelastic and electrically conducting fluid in a rotating vertical channel filled with the porous medium in the presence of magnetic field are:

Equation of Continuity

$$div\,\vec{V} = 0 \qquad (1)$$

Momentum Equation

$$\rho\left[\frac{\partial\vec{V}}{\partial t^*} + \vec{\Omega}\times\vec{V} + (\vec{V}\cdot\nabla)\vec{V}\right] = -\nabla p + \vec{j}\times\vec{B} + \mu\nabla^2\vec{V} - \frac{\mu}{K^*}\vec{V} + g\beta(T^* - T_0) + \nabla.\exists \qquad (2)$$

Energy Equation

$$\rho C_p\left[\frac{\partial T^*}{\partial t^*} + (\vec{V}.\nabla)T^*\right] = k\nabla^2 T^* - \nabla q \qquad (3)$$

Kirchhoffis First Law

$$div\,\vec{j} = 0 \qquad (4)$$

General Ohm’s Law

$$\vec{j} + \frac{\omega_e\tau_e}{B_0}(\vec{j}\times\vec{B}) = \sigma\left[\vec{E} + \vec{V}\times\vec{B} + \frac{1}{e\eta_e}\nabla p_e\right], \qquad (5)$$

Gauss’s Law of Magnetism

$$div\,\vec{B} = 0\,, \qquad (6)$$

Cauchy stress tensor Ǝ and the constitutive equation derived by Coleman and Noll (1960) for an incompressible homogeneous fluid of second grade is

$$\exists = -p_1 I + \mu_1 A_1 + \mu_2 A_2 + \mu_3 A_1^2. \qquad (7)$$

Here $-p_1{}^I$ is the interdeterminate part of the stress due to constraint of incompressibility, μ_1, μ_2 and μ_3 are the material constants describing viscosity, elasticity and cross-viscosity respectively. The kinematic A_1 and A_2 are the Rivelen Ericson constants defined as

$$A_1 = (\nabla\bar{V}) + (\nabla\bar{V})^T, \quad A_2 = \frac{dA_1}{dt} + (\nabla\bar{V})^T A_1 + A_1(\nabla\bar{V}),$$

where denotes the gradient operator and d/dt the material time derivative. According to Markovitz and Coleman (1964) the material constants μ_1, μ_3, are taken as positive and μ_2 as negative.

In the above equations vector *V* is the velocity vector, vector Ω is the angular velocity of the fluid, p is the pressure, ρ is the density, vector *B* is the magnetic induction vector, vector *j* is the current density, μ is the coefficient of viscosity, t* is the time, g is the acceleration due to gravity, β is the coefficient of volume expansion, K* is the permeability of the porous medium, Cp is the specific heat at constant pressure, T* is the temperature, T_o is the reference temperature that of the left plate, k is the thermal conductivity, q is the radiative heat, σ is the electrical conductivity, B_0 is the strength of the applied magnetic field, e is the electron charge, ωe is the electron frequency, τe is the electron collision time, pe is the electron pressure, vector *E* is the electric field and ηe is the number density of electron.

Formulation of the problem

Consider an unsteady MHD free convective flow of an electrically conducting, viscoelastic, incompressible fluid through a porous medium bounded between two insulated infinite vertical plates in the presence of Hall current and thermal radiation. The plates are at a distance 'd' apart. We introduce a Cartesian coordinate system with X*-axis oriented vertically upward along the centreline of the channel. The Z*- axis taken perpendicular to the planes of the plates lying in $z^* = \pm\frac{d}{2}$ planes is the axis of the rotation and the entire system rotates about this axis with uniform angular velocity Ω*. The fluid is injected through the porous plate at $z^* = -\frac{d}{2}$ with constant velocity w0 and simultaneous sucked through the other porous plate at $z^* = +\frac{d}{2}$ with the same velocity w0. The non-uniform temperature of the plate at $z^* = +\frac{d}{2}$ is assumed to be varying periodically with time. The temperature difference between the plates is high enough to induce the heat due to radiation. The diagram of the physical problem is shown below.

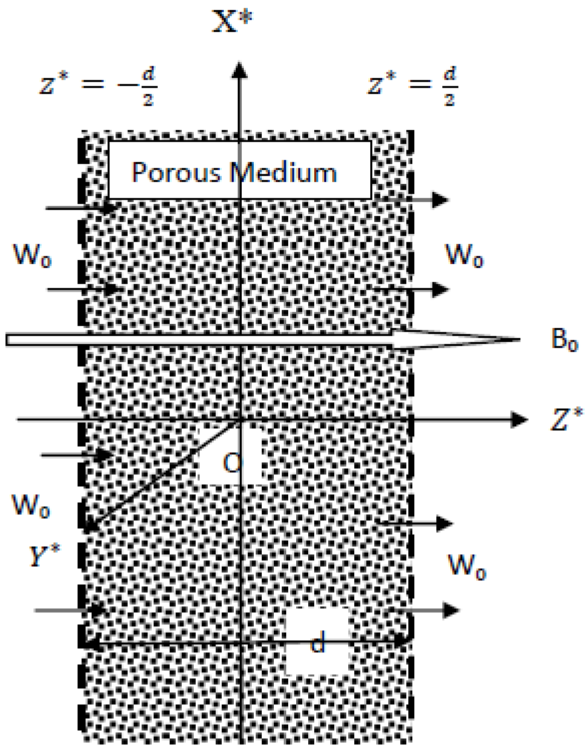

Figure 1: Schematic diagram of the physical problem

Since the plates of the channel are of infinite extent, all the physical quantities depend only on z* and t* only for this problem of fully developed laminar flow. Let *(u*, v*, w*)* be the components of velocity in the directions *(x*, y*, z*)* respectively. Since the plates are non-porous, therefore equation of continuity (1) on integration gives $w^* = 0$. A strong transverse magnetic field of uniform strength B_o is applied along the Z*-axis. So equation (6) for the magnetic field $\vec{B} = (B_x^*, B_y^*, B_z^*)$ gives $B_z^* = B_0$(constant).

If (j_x^*, j_y^*, j_z^*) are the components of electric current density vector j. The equation of conservation of electric charge gives j_z^*= constant. For non-conducting plates at the plates and hence zero everywhere in the fluid. Under the usual assumptions that the electron pressure (for a weakly ionized gas), the thermoelectric pressure, ion slip and the external electric field arising due to polarization of charges is negligible. It is assumed that no applied and polarization voltage exists. This corresponds to the case where no energy is being added or extracted from the fluid by electrical means (Meyer 1958) [21] i.e. electrical field vector E=0. Therefore, equation (5) takes the form:

$$\vec{j} + \frac{\omega_e \tau_e}{B_0}(\vec{j} \times \vec{B}) = \sigma(\vec{V} \times \vec{B}) \qquad (8)$$

After using equation $j_z^*=0$, equation (8) in component form becomes

$$j_x^* + \omega_e \tau_e\, j_y^* = \sigma B_0 v^* \qquad (9)$$

$$j_y^* - \omega_e \tau_e\, j_x^* = -\sigma B_0 u^* \qquad (10)$$

Solving (9) and (10) for j_x^* and j_y^*, we get

$$j_x^* = \frac{\sigma B_0}{(1+m^2)}(mu^* + v^*)$$

and

$$j_y^* = \frac{\sigma B_0}{(1+m^2)}(mv^* - u^*)$$

$H = \omega_e \tau_e$ is Hall parameter.

Under the usual Boussinsq's approximation and following Attia and Ewis (2010), Attia (2005), [22] Kumar and Khem (2011) [23] the momentum equation (2) and energy equation (3) reduce to

$$\frac{\partial u^*}{\partial t^*} + w_0 \frac{\partial u^*}{\partial z^*} - 2\Omega^* v^* = -\frac{1}{\rho}\frac{\partial p^*}{\partial x^*} + \vartheta_1 \frac{\partial^2 u^*}{\partial z^{*2}} + \vartheta_2 \frac{\partial^3 u^*}{\partial z^{*2}\partial t^*} + \frac{\sigma B_0^2 (Hv^* - u^*)}{\rho(1+H^2)} - \frac{\vartheta_1 u^*}{K^*} + g\beta(T^* - T_1) \qquad (11)$$

$$\frac{\partial v^*}{\partial t^*} + w_0 \frac{\partial v^*}{\partial z^*} + 2\Omega^* u^* = -\frac{1}{\rho}\frac{\partial p^*}{\partial y^*} + \vartheta_1 \frac{\partial^2 v^*}{\partial z^{*2}} + \vartheta_2 \frac{\partial^3 v^*}{\partial z^{*2}\partial t^*} - \frac{\sigma B_0^2 (Hu^* + v^*)}{\rho(1+H^2)} - \frac{\vartheta_1 u^*}{K^*} \qquad (12)$$

$$0 = -\frac{1}{\rho}\frac{\partial p^*}{\partial z^*} \qquad (13)$$

$$\frac{\partial T^*}{\partial t^*} + w_0 \frac{\partial T^*}{\partial z^*} = \frac{k}{\rho c_p}\frac{\partial^2 T^*}{\partial z^{*2}} - \frac{1}{\rho c_p}\frac{\partial q}{\partial z^*} \qquad (14)$$

where θ_2 is viscoelasticity and the last term in equation (14) is the radiative heat flux.

The boundary conditions for the flow problem are

$$u^* = L_1 \frac{\partial u^*}{\partial z^*},\ v^* = L_1 \frac{\partial v^*}{\partial z^*}\quad T^* = T_1 \ \text{at}\ z^* = -\frac{d}{2} \qquad (15)$$

$$u^* = v^* = 0,\ T^* = T_1 + (T_2 - T_1)\cos\omega^* t^* \ \text{at}\ z^* = \frac{d}{2} \qquad (16)$$

where $L_1 = \left(\frac{2-r_1}{r_1}\right)L,$, and ω^* is the frequency of oscillations.

Following Cogley et al. (1968) [24] it is assumed that the fluid is optically thin with a relatively low density and the heat flux due to radiation in equation (14) is given by

$$\frac{\partial q}{\partial z^*} = 4\alpha^2 (T^* - T_1), \qquad (17)$$

where α is the mean radiation absorption coefficient. After the substitution of equation (17) into equation (14), we get

$$\frac{\partial T^*}{\partial t^*}+w_0\frac{\partial T^*}{\partial z^*}=\frac{k}{\rho c_p}\frac{\partial^2 T^*}{\partial z^{*2}}-\frac{4\alpha^2}{\rho c_p}(T^*-T_1) \tag{18}$$

Equation (13) shows the constancy of the hydrodynamic pressure along the axis of rotation. We shall assume now that the fluid flows under the influence of pressure gradient varying periodically with time in the X*-axis is of the form

$$-\frac{1}{\rho}\frac{\partial p^*}{\partial x^*}=A\cos\omega^* t^* \text{ and } -\frac{1}{\rho}\frac{\partial p^*}{\partial y^*}=0,$$ where A is a constant. (19)

Introducing the following non-dimensional quantities

$$\eta=\frac{z^*}{d},\ x=\frac{x^*}{d},\ y=\frac{y^*}{d},\ u=\frac{u^*}{w_0},\ v=\frac{v^*}{w_0},\ T=\frac{T^*-T_1}{T_2-T_1},\ t=\frac{t^* w_0}{d},\ \omega=\frac{\omega^* d}{w_0},\ \Omega=\frac{\Omega^* d^2}{\vartheta_1},$$
$$p=\frac{p^*}{\rho w_0^{\,2}}$$

Into equations (11), (12), and (18), we get

$$\lambda\left(\frac{\partial u}{\partial t}+\frac{\partial u}{\partial \eta}\right)=-\lambda\frac{\partial p}{\partial x}+\frac{\partial^2 u}{\partial \eta^2}+\gamma\frac{\partial^3 u}{\partial \eta^2\partial t}+2\Omega v+\frac{M^2(Hv-u)}{(1+H^2)}-K^{-1}u+Gr\,T \tag{20}$$

$$\lambda\left(\frac{\partial v}{\partial t}+\frac{\partial v}{\partial \eta}\right)=-\lambda\frac{\partial p}{\partial y}+\frac{\partial^2 v}{\partial \eta^2}+\gamma\frac{\partial^3 v}{\partial \eta^2\partial t}-2\Omega u-\frac{M^2(Hu+v)}{(1+H^2)}-K^{-1}v \tag{21}$$

$$\lambda Pr\left(\frac{\partial T}{\partial t}+\frac{\partial T}{\partial \eta}\right)=\frac{\partial^2 T}{\partial \eta^2}-N^2T \tag{22}$$

where ‘*’ represents the dimensional physical quantities,

$\lambda=\frac{w_0 d}{\vartheta_1}$ is the injection/suction parameter,

$\gamma=\frac{\upsilon_2\lambda}{d^2}$ is the visco-elastic parameter,

$M=B_0 d\sqrt{\frac{\sigma}{\rho\vartheta_1}}$ is the Hartmann number,

$H=\omega_e\tau_e$ is the Hall parameter,

$K=\frac{K^*}{d^2}$ is the permeability of the porous medium,

$Gr=\frac{g\beta d^2(T_2-T_1)}{\vartheta_1 w_0}$ is the Grashof number,

$Pr=\frac{\rho\vartheta_1 c_p}{k}$ is the Prandtl number,

$N=\frac{2\alpha d}{\sqrt{k}}$ is the radiation parameter,

$\Omega=\frac{\Omega^* d^2}{\vartheta_1}$ is the rotation parameter,

$\omega=\frac{\omega^* d}{w_0}$ is the frequency of oscillations.

The corresponding transformed boundary conditions are:

$$u = h\frac{\partial u}{\partial \eta}, v = h\frac{\partial v}{\partial \eta}, T = 0 \; at \; \eta = -\frac{1}{2} \tag{24}$$

$$u = v = 0, T = \cos\omega t \; at \; \eta = \frac{1}{2} \tag{25}$$

where $h = L_1/d$ is the slip-flow parameter.

For the oscillatory internal flow we shall obtained from equation (19) that the fluid flows only under the influence of a non-dimensional pressure gradient oscillating in time in the direction of x-axis only which is of the form

$$-\frac{\partial p}{\partial x} = A\cos\omega t \text{ and } -\frac{\partial p}{\partial y} = 0 \tag{26}$$

Solution to the problem

In order to combine equations (20) and (21) into single equation, we introduce a complex function and using (26), we get

$$\lambda\left(\frac{\partial F}{\partial t} + \frac{\partial F}{\partial \eta}\right) = -\lambda\frac{\partial p}{\partial x} + \frac{\partial^2 F}{\partial \eta^2} + \gamma\frac{\partial^3 F}{\partial \eta^2 \partial t} - 2i\Omega F - \left(\frac{M^2(1+iH)}{(1+H^2)} + K^{-1}\right)F + Gr\,T \tag{27}$$

The boundary conditions (24) and (25) in complex notation can be written as:

$$F = h\frac{\partial F}{\partial \eta}, \; T = 0 \; at \; \eta = -\frac{1}{2}, \tag{28}$$

$$F = 0, \; T = \cos\omega t \; at \; \eta = \frac{1}{2} \tag{29}$$

In order to solve equations (27) and (22) under the boundary conditions (28) and (29), we assume in complex form the solution of the problem as:

$$F(\eta,t) = F_0(\eta)e^{i\omega t}, T(\eta,t) = \theta_0(\eta)e^{i\omega t} \text{ and } -\frac{\partial p}{\partial x} = Ae^{i\omega t} \tag{30}$$

where only the real part of the solution is significant.

Substituting equation (4.30) in equations (4.27) and (4.22), we get

$$(1 + i\omega\gamma)\frac{d^2F_0}{d\eta^2} - \lambda\frac{dF_0}{d\eta} - \left\{\frac{M^2(1+iH)}{(1+H^2)} + 2i\Omega + K^{-1} + i\omega\lambda\right\}F_0 = -\lambda A - Gr\,\theta_0 \tag{31}$$

$$\frac{d^2\theta_0}{d\eta^2} - \lambda Pr\frac{d\theta_0}{d\eta} - (N^2 + i\omega\lambda Pr)\theta_0 = 0 \tag{32}$$

The corresponding boundary conditions (28) and (29) become:

$$F_0 = h\frac{\partial F_0}{\partial \eta}, \theta_0 = 0 \; at \; \eta = -\frac{1}{2}, \tag{33}$$

$$F_0 = 0, \theta_0 = 1 \; at \; \eta = \frac{1}{2}. \tag{34}$$

The solution of the ordinary differential equation (31) for the velocity field under the boundary conditions (33) and (34) is obtained as

$$F(\eta,t)=\left[\begin{array}{c}\frac{\lambda A}{l}\left\{1+\frac{\left((1-hm)e^{-\frac{m}{2}}-e^{\frac{m}{2}}\right)e^{n\eta}-\left((1-hn)e^{-\frac{n}{2}}-e^{\frac{n}{2}}\right)e^{m\eta}}{(1-hn)e^{\frac{m-n}{2}}-(1-hm)e^{-\frac{m-n}{2}}}\right\}+\\ \frac{Gr}{2\sinh\left(\frac{r-s}{2}\right)}\left\{\begin{array}{c}\left(\frac{e^{\frac{r-s}{2}}}{C_1}-\frac{e^{-\frac{r-s}{2}}}{C_2}\right)\left(\frac{(1-hn)e^{m\eta-\frac{n}{2}}-(1-hm)e^{n\eta-\frac{m}{2}}}{(1-hn)e^{\frac{m-n}{2}}-(1-hm)e^{-\frac{m-n}{2}}}\right)\\ +\left(\frac{1-hs}{C_2}-\frac{1-hr}{C_1}\right)\left(\frac{e^{m\eta+\frac{n}{2}}-e^{n\eta+\frac{m}{2}}}{(1-hn)e^{\frac{m-n}{2}}-(1-hm)e^{-\frac{m-n}{2}}}\right)e^{-\frac{\lambda Pr}{2}}\end{array}\right\}\\ -\frac{Gr}{2\sinh\left(\frac{r-s}{2}\right)}\left(\frac{e^{r\eta-\frac{s}{2}}}{C_1}-\frac{e^{s\eta-\frac{r}{2}}}{C_2}\right)\end{array}\right]e^{i\omega t}$$

(35)

$$C_1=(1+i\omega\gamma)r^2-\lambda r-l\,,\quad C_2=(1+i\omega\gamma)s^2-\lambda s-l,$$

$$l=\frac{M^2(1+iH)}{(1+H^2)}+2i\Omega+K^{-1}+i\omega\lambda\,,$$

$$m=\frac{\lambda+\sqrt{\lambda^2+4l(1+i\omega\gamma)}}{2(1+i\omega\gamma)}\,,\qquad n=\frac{\lambda-\sqrt{\lambda^2+4l(1+i\omega\gamma)}}{2(1+i\omega\gamma)}\,,$$

$$r=\frac{\lambda Pr+\sqrt{\lambda^2Pr^2+4(N^2+i\omega\lambda Pr)}}{2}\,,\qquad s=\frac{\lambda Pr-\sqrt{\lambda^2Pr^2+4(N^2+i\omega\lambda Pr)}}{2}$$

Similarly, the solution of equation (32) for the temperature field under the boundary conditions (33) and (34) is obtained as

$$T(y,t)=\left(\frac{e^{r\eta-\frac{s}{2}}-e^{s\eta-\frac{r}{2}}}{2\sinh\left(\frac{r-s}{2}\right)}\right)e^{i\omega t}$$

(36)

From the velocity field obtained in equation (35) we can get the skin-friction at the left plate (η = - 0.5) in terms of its amplitude |F| and phase angle φ as

$$\tau=\left(\frac{\partial u}{\partial y}\right)_{y=-\frac{1}{2}}=|F|\,\cos(t+\varphi)$$

, with (37)

$$F=F_r+i\,F_i=\left[\begin{array}{c}\frac{\lambda A}{l}\left(\frac{n\left((1-hm)e^{-\frac{m}{2}}-e^{\frac{m}{2}}\right)e^{-\frac{n}{2}}-m\left((1-hn)e^{-\frac{n}{2}}-e^{\frac{n}{2}}\right)e^{-\frac{m}{2}}}{(1-hn)e^{\frac{m-n}{2}}-(1-hm)e^{-\frac{m-n}{2}}}\right)+\\ \frac{Gr}{2\sinh\left(\frac{r-s}{2}\right)}\left\{\begin{array}{c}\left(\frac{e^{\frac{r-s}{2}}}{C_1}-\frac{e^{-\frac{r-s}{2}}}{C_2}\right)\left(\frac{m(1-hn)-n(1-hm)}{(1-\delta n)e^{\frac{m-n}{2}}-(1-\delta m)e^{-\frac{m-n}{2}}}\right)e^{-\frac{\lambda}{2(1+i\omega\gamma)}}\\ +\left(\frac{1-hs}{C_2}-\frac{1-hr}{C_1}\right)\left(\frac{me^{-\frac{m-n}{2}}-ne^{\frac{m-n}{2}}}{(1-hn)e^{\frac{m-n}{2}}-(1-hm)e^{-\frac{m-n}{2}}}\right)e^{-\frac{\lambda Pr}{2}}\end{array}\right\}\\ -\frac{Gr}{2\sinh\left(\frac{r-s}{2}\right)}\left(\frac{r}{C_1}-\frac{s}{C_2}\right)e^{-\frac{\lambda Pr}{2}}\end{array}\right]$$

(38)

The amplitude is $|F|=\sqrt{F_r^2+F_i^2}$ and the phase angle $\varphi=\tan^{-1}\frac{F_i}{F_r}.$ (39)

Similarily, we can get the Nusselt number Nu for the rate of heat transfer, in terms of its amplitude |H| and the phase angle ψ from equation (36) for the temperature field as

$$Nu = |H| \cos(t + \psi), \quad \text{with} \quad H = H_r + iH_i = \frac{(r-s)e^{\frac{\lambda Pr}{2}}}{2\sinh\left(\frac{r-s}{2}\right)}, \tag{40}$$

where the amplitude |H| and the phase angle ψ of the rate of heat transfer are given as

$$|H| = \sqrt{H_r^{\,2} + H_i^{\,2}}, \qquad \psi = \tan^{-1}\frac{H_i}{H_r}. \tag{41}$$

The temperature field, the rate of heat transfer along with its amplitude and phase angle need no discussion because these have already been discussed in detail by Singh (2013) [24].

Results and discussion

The problem of oscillatory magnetohydrodynamic (MHD) convective and radiative flow in a vertical porous channel is analyzed in the slip-flow regime. The viscoelastic, incompressible and electrically conducting fluid is injected through one of the porous plates and simultaneously removed through the other porous plate with the same velocity. The entire system (consisting of Porous channel plates and the fluid) rotates about an axis perpendicular to the plates. The closed form solutions for the velocity and temperature fields are obtained analytically and then evaluated numerically for different values of parameters appeared in the equations. To have better insight of the physical problem the variations of the velocity, the skin-friction in terms of its amplitude and phase angle are evaluated numerically for different sets of the values of injection/suction parameter ƛ, viscoelastic parameter γ, rotation parameter Ω, Hartmann number M, Hall parameter H, the permeability parameter K, Grashof number Gr, Prandtl number Pr, radiation parameter N, pressure gradient A and the frequency of oscillations ω. These numerical values are then shown graphically to assess the effect of each parameter for the two cases of rotation Ω = 5 (small) and Ω = 15 (large). The velocity variations are presented graphically in figs. 4.2 to 4.11 for h = 0.5, γ=0.2, =0.5, Gr=5, M=2, H = 1, K=0.2, Pr=0.7, N=1, A=5, =5 and t=0 except the ones shown in these figures.

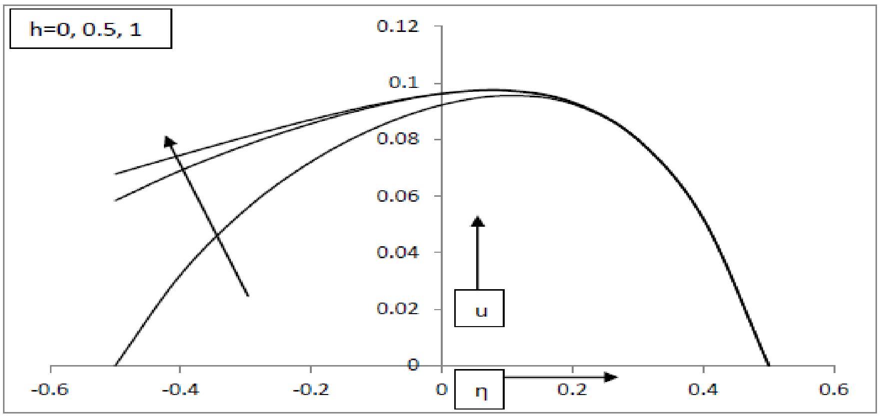

Figure 2: Velocity variation with increasing slip-flow parameter h keeping other parameters fixed as Ω=5, γ=0.2, ƛ=0.5, Gr=5, M=2, H = 1, K=0.2, Pr=0.7, N=1, A=5, ω=5 and t=0

Fig. 2 illustrates the variation of the velocity with the increasing slip-flow parameter h. It is quite obvious from this figure that velocity goes on increasing with increasing slip-flow parameter h.

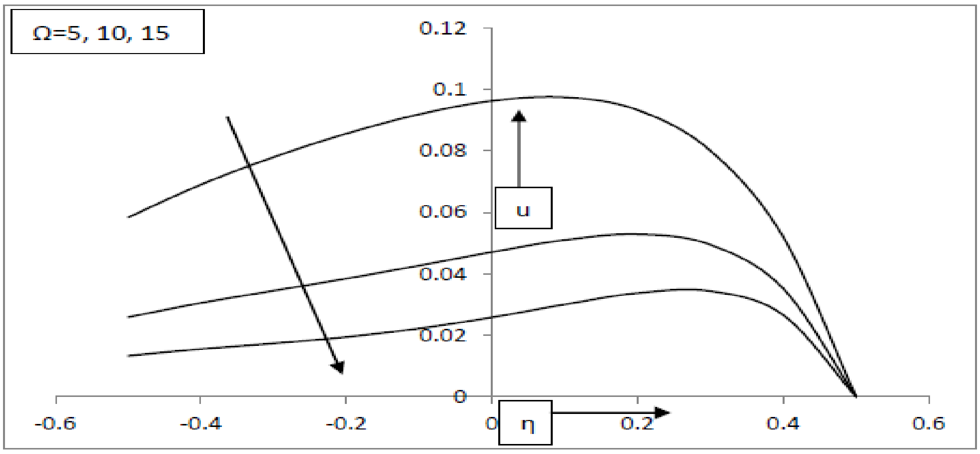

Figure 3: Velocity variation with increasing rotation parameter Ω keeping other parameters fixed as h=0.5, γ=0.2, ƛ=0.5, Gr=5, M=2, H = 1, K=0.2, Pr=0.7, N=1, A=5, ω=5 and t=0

The velocity variations with the rotation parameter Ω are presented in Fig.3. The velocity decreases with increasing rotation Ω of the entire system. The velocity profiles initially remain parabolic for small values of rotation parameter Ω with a maximum near the centre of the channel and then as rotation increases the velocity profiles flatten and the maximum shifts towards the plate with the no-slip condition.

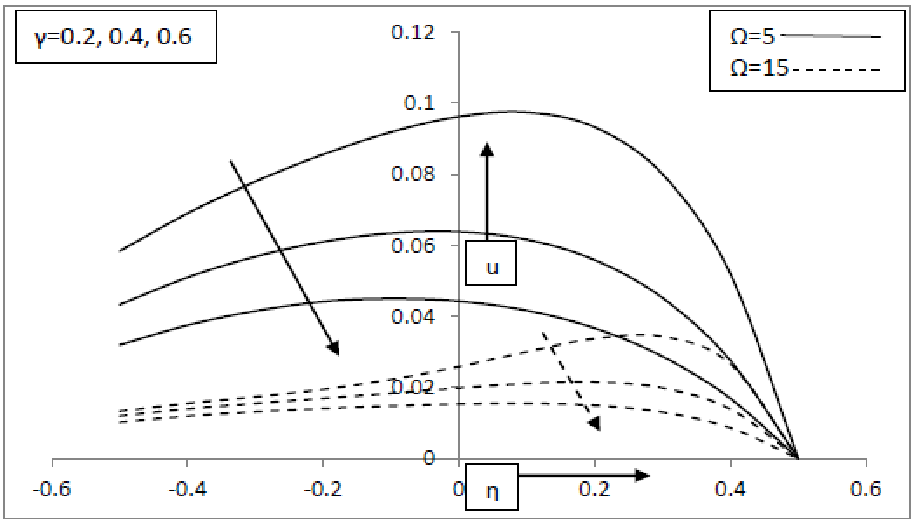

Figure 4: Velocity variation with increasing visco-elastic parameter γ keeping other parameters fixed as h=0.5, =0.5, Gr=5, M=2, H = 1, K=0.2, Pr=0.7, N=1, A=5, ω=5 and t=0

The variations of the velocity profiles with the viscoelastic parameter γ are presented in Fig.4. It is very clear from this figure that the velocity decreases with the increase of viscoelastic parameter for both the cases of small (Ω = 5) and large (Ω = 15) rotations of the channel.

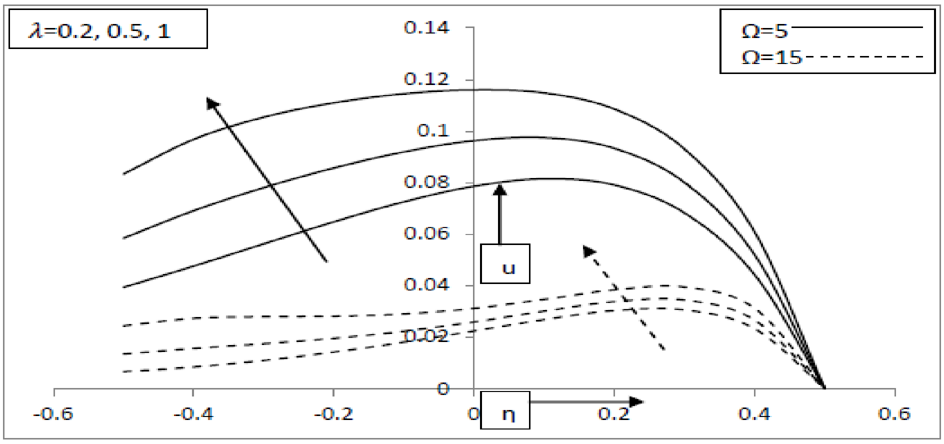

Figure 5: Velocity variation with increasing injection/suction parameter keeping other parameters fixed as h=0.5, γ=0.2, Gr=5, M=2, H = 1, K=0.2, Pr=0.7, N=1, A=5, ω=5, t=0

However, for both these cases of rotation, the velocity increases significantly with increasing injection/suction parameter as is revealed in Fig.5.

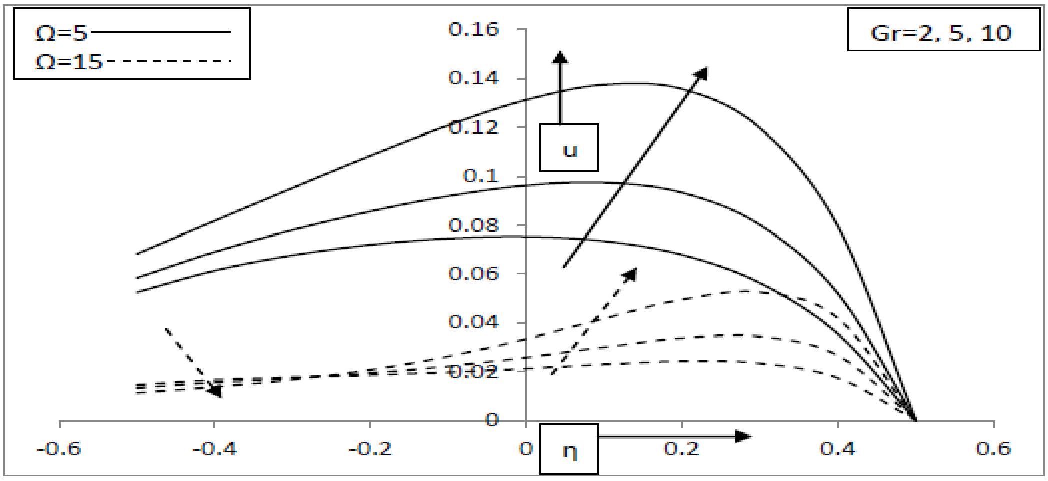

Figure 6: Velocity variation with increasing Grashof number Gr keeping other parameters fixed as h=0.5, γ=0.2, λ=0.5, M=2, H = 1, K=0.2, Pr=0.7, N=1, A=5, ω=5 and t=0

The variations of the velocity profiles with the Grashof number Gr are presented in Fig.6. It is observed that for small (Ω=5) rotation of the channel the velocity increases with increasing Grashof number. However, for large rotations (Ω=15) the velocity increases with Gr in the right half of the channel wherein hotter plate lies but decreases in the left half of the channel. For small and large rotations both the maximum of the velocity profiles shifts in the right half of the channel due to the greater buoyancy force in this part of the channel because of the presence of hotter plate. The Grashof number has opposite effect on the velocity profiles in the right half and the left half of the channel. In the right half there lies hot plate at η = 1/2 and heat is transferred from the hot plate to the fluid and consequently buoyancy force enhances the flow velocity further. In the left half of the channel the transfer of heat takes place from the fluid to the cooler plate at η = -1/2. Thus, the effect of Grashof number on the velocity is reversed i.e. velocity decreases in the left half of the channel with increasing Gr.

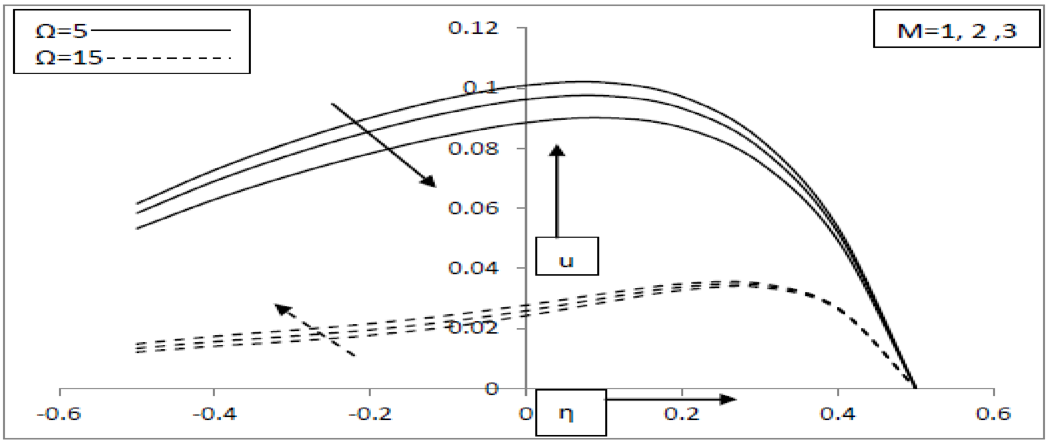

Figure 7: Velocity variation with increasing Hartmann number M keeping other parameters fixed as h=0.5, γ=0.2, λ=0.5, Gr=5, H = 1, K=0.2, Pr=0.7, N=1, A=5, ω=5 and t=0

It is evident from the Fig. 7 that for small rotation (Ω=5) the velocity decreases with the increase of Hartmann number M. This is because of the reason that effects of a transverse magnetic field on an electrically conducting fluid gives rise to a resistive type force (called Lorentz force) similar to drag force and upon increasing the values of M increases the drag force which has a tendency to slow down the motion of the fluid. However, for large rotations (Ω=15) the effect of Hartmann number is reversed because decreasing velocity due to the larger rotation is resisted by the Lorentz force.

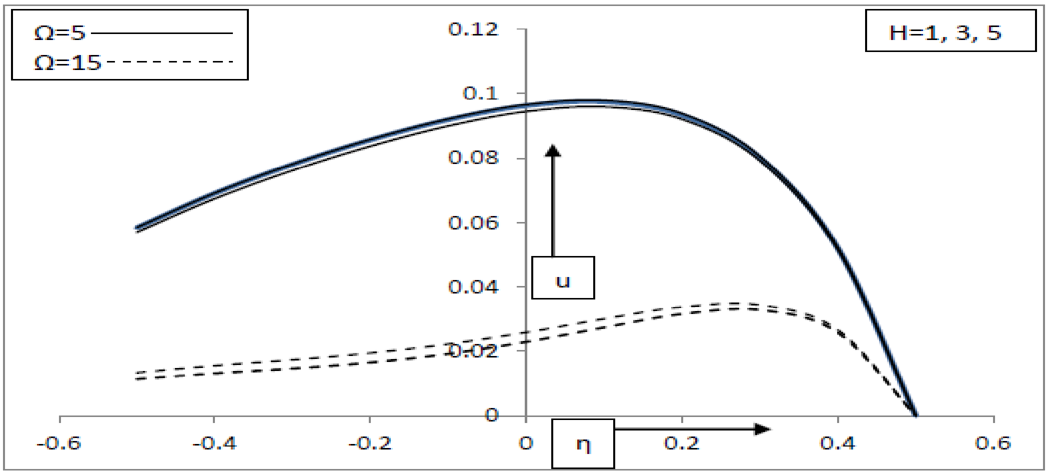

Figure 8: Velocity variation with increasing Hall parameter H keeping other parameters fixed as h=0.5, γ=0.2, λ=0.5, Gr=5, M=2, K=0.2, Pr=0.7, N=1, A=5, ω=5 and t=0

Fig.8 depicts the variation of the velocity with Hall parameter H. The effect of Hartmann number on the velocity is insignificant for small or large rotations of the channel.

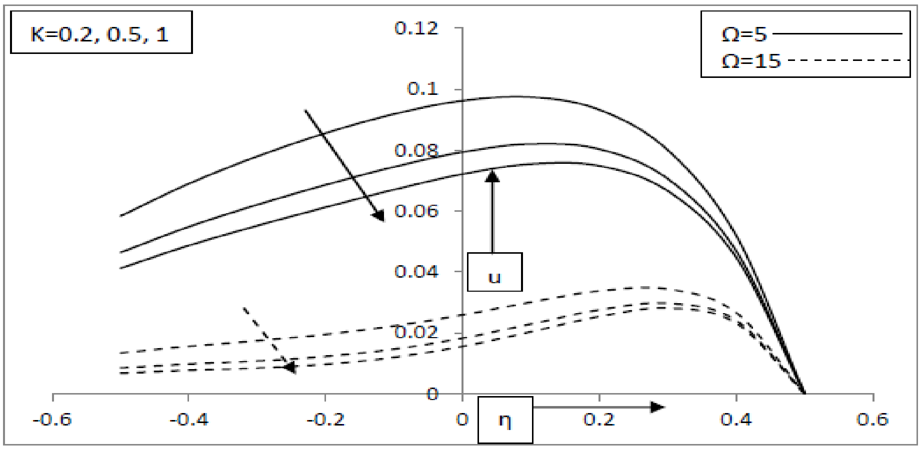

Figure 9: Velocity variation with increasing permeability parameter K keeping other parameters fixed as h=0.5, γ=0.2, λ=0.5, Gr=5, M=2, H=1, Pr=0.7, N=1, A=5, ω=5 and t=0.

The variation of the velocity with the permeability of the porous medium K is shown in Fig. 9. It is observed from the figure that the velocity decreases with the increasing permeability K of the porous medium for both small (Ω=5) and large (Ω=15) rotations of this system of the viscoelastic fluid flow. It is expected physically also because the resistance posed by the porous medium to the decelerated flow due to rotation reduces with increasing permeability K which lead to decrease in the velocity. For Ω=15 velocity is much less than Ω=5.

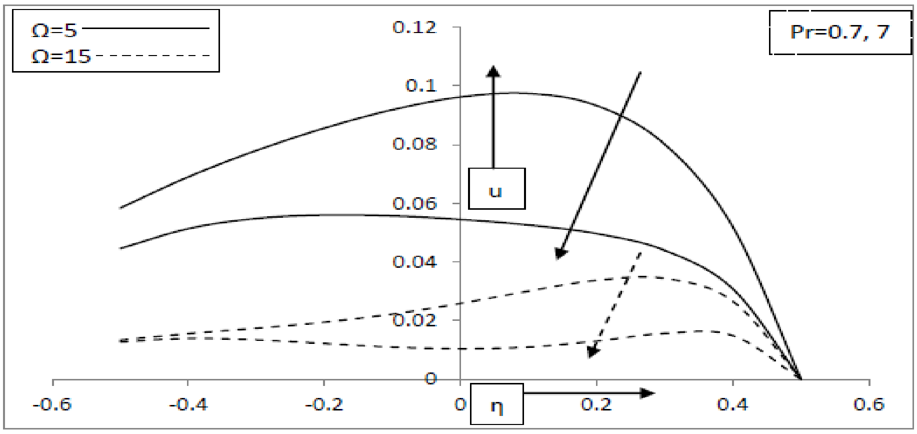

Figure 10: Velocity variation with increasing Prandtl number Pr keeping other parameters fixed as h=0.5, γ=0.2, λ=0.5, Gr=5, M=2, H=1, K=0.2, N=1, A=5, ω=5 and t=0

We find from Fig.10 that with the increase of Prandtl number Pr and the radiation parameter N the velocity decreases for small (Ω=5) and large (Ω=15) rotations both.

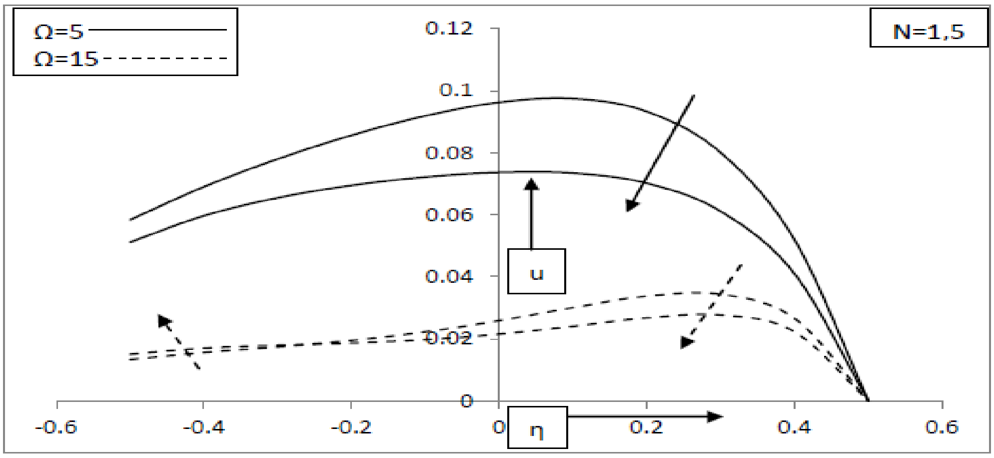

Figure 11: Velocity variation with increasing radiation parameter N keeping other parameters fixed as h=0.5, γ=0.2, λ=0.5, Gr=5, M=2, H=1, K=0.2, Pr=0.7, A=5, ω=5 and t=0

We also infer from Fig.11 that the velocity decreases with increasing radiation parameter N for small rotation (Ω=5). However, for large rotation (Ω=15) the radiation parameter has an opposing effect on the velocity, i.e., the velocity decreases in the right half and increases slightly in the left half of the channel.

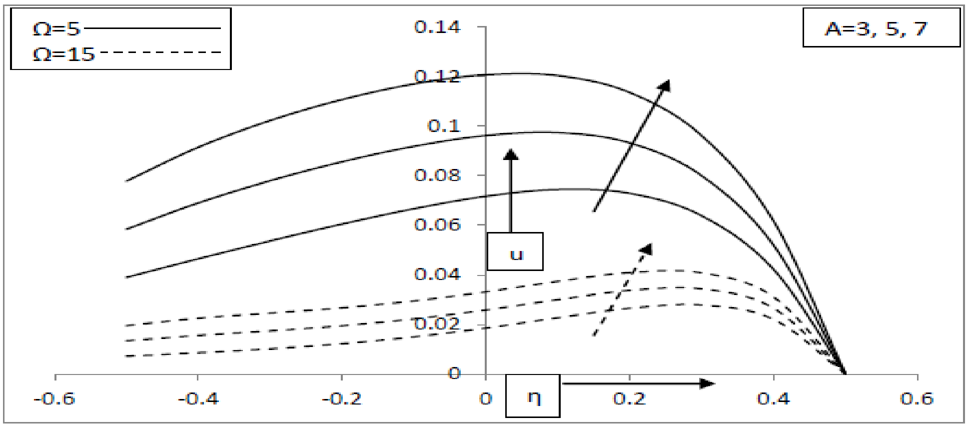

Figure 12: Velocity variation with increasing pressure gradient A keeping other parameters fixed as h=0.5, γ=0.2, λ=0.5, Gr=5, M=2, H=1, K=0.2, Pr=0.7, N=1, ω=5 and t=0

From Fig.12 it is evident that the velocity goes on increasing with the increasing favourable pressure gradient P (>0).

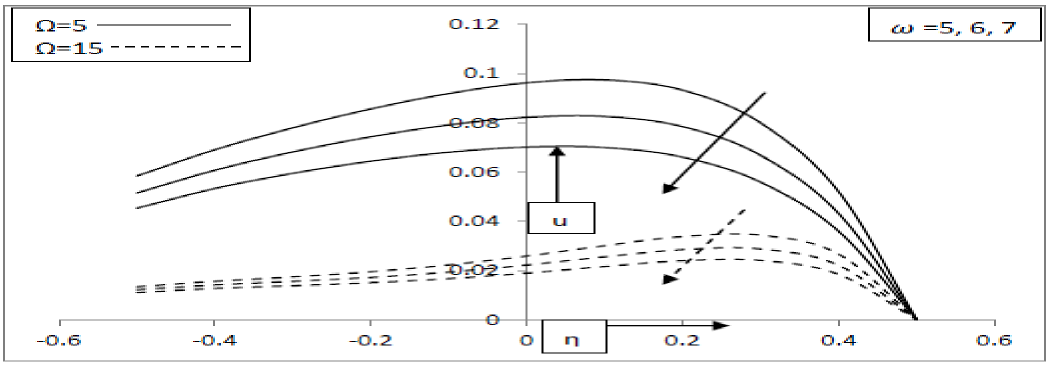

Figure 13: Velocity variation with increasing frequency of oscillations ω keeping other parameters fixed as h=0.5, γ=0.2, λ=0.5, Gr=5, M=2, H=1, K=0.2, Pr=0.7, N=1, A=5, t=0

The effects of the frequency of oscillations on the velocity are exhibited in Fig.13. It is noticed that velocity decreases with increasing frequency for either case of channel rotation large or small.

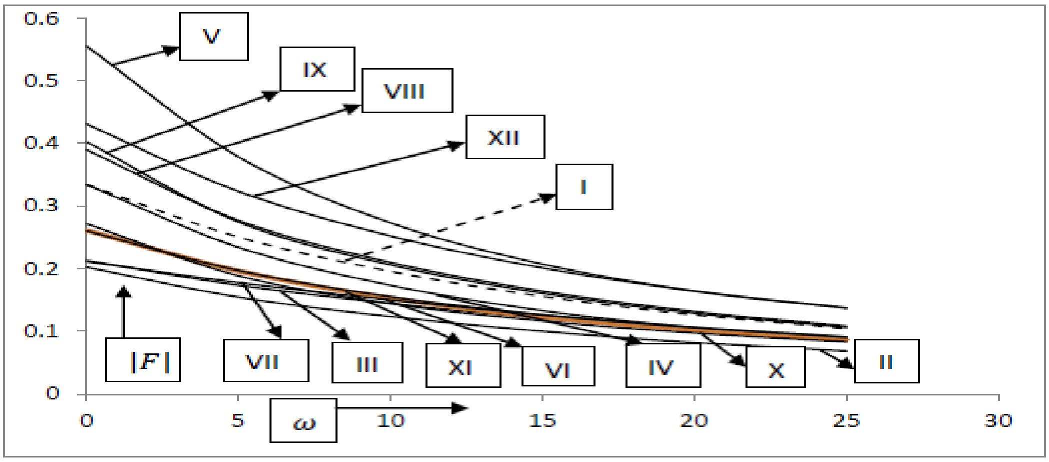

Figure 14: Amplitude of the skin-friction for values of the parameters in Table 1

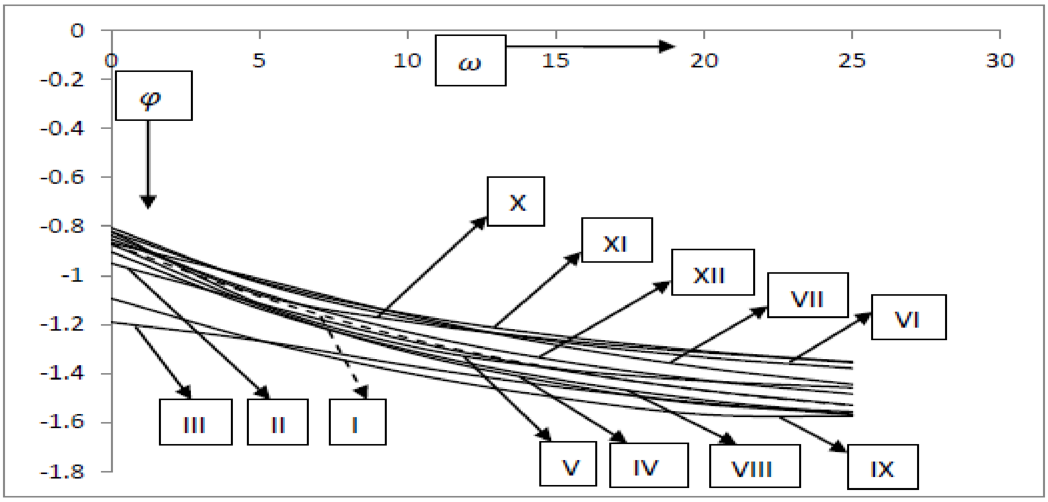

Figure 15: Phase of the skin-friction for values of the parameters in Table 4.1

The skin-friction in terms of its amplitude and phase angle has been shown in Figs.14 and 15 respectively. The effect of each of the parameter on and is assessed by comparing each curve with dotted curves in these figures. In Fig.13 the comparison of the curves V, VIII, IX, and XII with dotted curve I (-----) indicate that the amplitude increases with the increase of injection/suction parameter ƛ, Hall parameter H, permeability of the porous medium K and pressure gradient A.

Table 1: Values of parameters plotted in Figs.14 & 15

h	Ω	γ	λ	Gr	M	H	K	Pr	N	A	Curves
0.5	5	0.2	0.5	5	2	1	0.2	0.7	1	5	I ( )
1.0	5	0.2	0.5	5	2	1	0.2	0.7	1	5	II
0.5	10	0.2	0.5	5	2	1	0.2	0.7	1	5	III- - -
0.5	5	0.3	0.5	5	2	1	0.2	0.7	1	5	IV
0.5	5	0.2	1.0	5	2	1	0.2	0.7	1	5	V
0.5	5	0.2	0.5	10	2	1	0.2	0.7	1	5	VI
0.5	5	0.2	0.5	5	4	1	0.2	0.7	1	5	VII
0.5	5	0.2	0.5	5	2	5	0.2	0.7	1	5	VIII
0.5	5	0.2	0.5	5	2	1	1.0	0.7	1	5	IX
0.5	5	0.2	0.5	5	2	1	0.2	7.0	1	5	X
0.5	5	0.2	0.5	5	2	1	0.2	0.7	5	5	XI
0.5	5	0.2	0.5	5	2	1	0.2	0.7	1	7	XII

Similarly, the comparison of other curves II, III, IV, VI, VII, X, and XI with the dotted curve I (----) reveals that the skin-friction amplitude decreases with the increase of slip flow parameter h, rotation parameter Ω, viscoelastic parameter γ, Grashof number Gr, Hartmann number M, Prandtl number Pr and the radiation parameter N. It is obvious that goes on decreasing with increasing frequency of oscillations ω. Fig. 4.14 showing the variations of the phase angle φ of the skin-friction it is clear that there is always a phase lag because the values of φ remains negative throughout. Here again the comparison of curves II, III, IV, V, VIII, and IX with the dotted curve I (---) indicate that the phase lag increases with the increase of slip-flow parameter h, rotation parameter Ω, viscoelastic parameter γ, injection/suction parameter ƛ, Hall parameter H and permeability of the porous medium K. The comparison of other curves like VI, VII, X, XI, and XII with the dotted curve (---) I shows that the phase lag decreases with the increase of Grashof number Gr, Hartmann number M, Prandtl number Pr, radiation parameter N and the pressure gradient parameter A.

Conclusion

An oscillatory magnetohydrodynamic (MHD) convective flow of an electrically conducting viscoelastic fluid in a vertical rotating channel is studied analytically in the slip-flow regime. The pressure gradient and the temperature of one of the plates of the channel vary periodically with time. A strong magnetic field is applied along the axis of rotation, and the Hall currents are taken into account. Results are presented graphically for two cases of small rotation (Ω=5), and large rotation (Ω=15) and some following important conclusions are drawn from these figures:

a. The velocity increases with the- increase of slip-flow parameter.

b. The velocity decreases with increasing rotation of the system. For small rotation the velocity profiles are nearly parabolic with the maximum nearly at the centre of the channel but as the rotation increases the maximum shifts towards the walls with the no-slip condition.

c. The velocity decreases with the increasing viscoelasticity of the fluid irrespective that the rotation is small or large.

d. For rotation small or large, the velocity increases significantly with increasing injection/suction parameter.

e. For small rotation of the channel, the velocity increases with increasing Grashof number. However, for large rotations, the Grashof number has an opposing effect on the velocity i.e., velocity increases in that part of the channel where the heat is transferred from the channel wall to the fluid but decreases where the heat is transferred from the fluid to the channel wall.

f. The increasing magnetic field strength and the permeability of the porous medium retard the forward and the backward flows for the cases of small and large rotations.

g. The velocity decreases with the increase of Prandtl number and the radiation parameter.

h. The velocity increases with the increase of favourable pressure gradient but decreases with increasing frequency of oscillations.

i. The amplitude |F| increases with the increase of injection/suction parameter ƛ, Hall parameter H, permeability of the porous medium K and pressure gradient A but decreases with the increase of slip flow parameter h, rotation parameter Ω, viscoelastic parameter γ, Grashof number Gr, Hartmann number M, Prandtl number Pr and the radiation parameter N.

j. There is always a phase lag. The phase lag increases with the increase of slip-flow parameter h, rotation parameter Ω, viscoelastic parameter γ, injection/suction parameter ƛ, Hall parameter H and permeability of the porous medium K but decreases with the increase of Grashof number Gr, Hartmann number M, Prandtl number Pr, radiation parameter N and the pressure gradient parameter A.

References

[1] Singh, K. D., (2000), "An Oscillatory Hydromagnetic Couette Flow in a Rotating System," ZAMM-Journal of Applied Mathematics and Mechanics., **80(6)**, pp. 429-432.

[2] Singh, K. D., (2013), "Exact Solution of Mhd Mixed Convection Periodic Flow in a Rotating Vertical Channel with Heat Radiation," International Journal of Applied Mechanics and Engineering., **18(3)**, pp. 853-869.

[3] Hassanien, I. A., and Mansour, M. A., (1990), "Unsteady Magnetohydrodynamic Flow Through a Porous Medium Between Two Infinite Parallel Plates," Astrophysics and Space Science., **163(2)**, pp. 241-246.

[4] Hayat, T., Asghar, S., and A. M. Siddiqui, A. M., (1998), "Periodic Unsteady Flows of a Non-Newtonian Fluid," Acta Mechanica., **131(3-4)**, pp. 169-175.

[5] Choudhury, R., and Das, U. J., (2012), "Heat Transfer to Mhd Oscillatory Viscoelastic Flow in a Channel Filled with Porous Medium," Hindawi Publishing Corporation-Physics Research International, Article ID 879537., 2012, pp. 1-5.

[6] Singh, K. D., (2012), "Visco-Elastic Mixed Convection Mhd Oscillatory Flow Through a Porous Medium Filled in a Vertical Channel," International Journal of Physical and Mathematical Sciences., **3(1)**, pp. 194-205.

[7] Hayat, T., Nadeem, S., and Asghar, S., (2004), "Hydromagnetic Couette Flow of an Oldroyd-B Fluid in a Rotating System," International Journal of Engineering Science., **42(1)**, pp. 65-78.

[8] Hayat, T., Hutter, K., Nadeem, S., and Asghar, S., (2004), "Unsteady Hydromagnetic Rotating Flow of a Conducting Second Grade Fluid," ZAMP-Journal of Applied Mathematics and Physics., **55(4)**, pp. 626-641.

[9] Rahman, M. M., and Sarkar, M. S. A., (2004), "Unsteady Mhd Flow of Visco-Elastic Oldroyd Fluid Under Time Varying Body Forces Through a Rectangular Channel," Bulletin of Calcutta Mathematical Society., **96(6)**, pp. 463-470.

[10] Rajagopal, K., Veena, P. H., and Pravin, V. K., (2006), "Oscillatory Motion of an Electrically Conducting Viscoelastic Fluid Over a Stretching Sheet in a Saturated Porous Medium with Suction/Blowing," Hindawi Publishing Corporation-Mathematical Problems in Engineering, Article ID 60560., 2006, pp. 1-14.

[11] Prasuna, T. G., Murthy, M. V. R., Ramacharyulu, N. C. P., and Rao, G. V., (2010), "Unsteady Flow of a Viscoelastic Fluid Through a Porous Media Between Two Impermeable Parallel Plates," Journal of Emerging Trends in Engineering and Applied Sciences., **1(2)**, pp. 225-229.

[12] Attia, H. A., (1998), "Hall Current Effects on Velocity and Temperature Fields of an Unsteady Hartmann Flow," Canadian Journal of Physics, **76(9)**, pp. 739-746.

[13] Garg, B. P., and Singh, K. D., (2010), "Exact Solution of an Oscillatory Heat and Mass Transfer Mixed Convection Flow in a Rotating Channel with Heat Source/Sink and Soret Effect," Proceedings of the National Academy of Sciences India Section A-Physical Sciences **80(4)**, pp. 347-356.

[14] Marques, Jr. W., Kermer, G. M., and Sharipov, F. M., (2000), "Couette Flow with Slip and Jump Boundary Conditions," Continuum Mechanics and Thermodynamics., **12(6)**, pp. 379-386.

[15] Rhodes, C. A., and Rouleau, W. T., (1966), "Hydromagnetic Lubrication of Partial Porous Metal Bearings," ASME-Journal of Fluids Engineering., **88(1)**, pp. 53- 60.